Cell Reports

Resource

MouSensor: A Versatile Genetic Platform to Create Super Sniffer Mice for Studying Human Odor Coding

Graphical Abstract

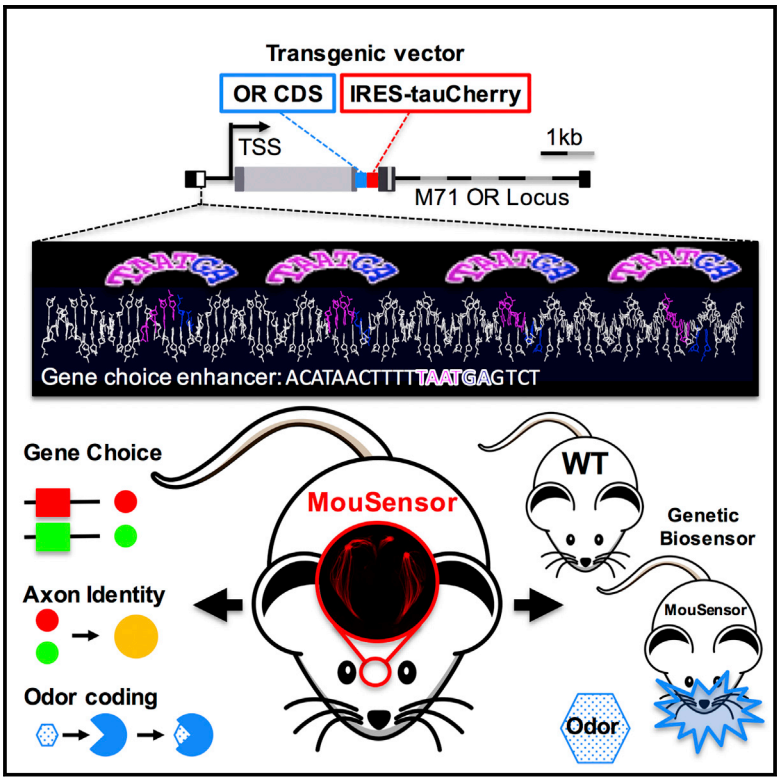

Highlights

- Odorant receptor expression can be controlled using a 21-bp gene choice enhancer
- In vivo synaptopHluorin imaging shows functional glomerular activation in MouSensors
- MouSensors show lower specific odorant detection thresholds
- Human odorant receptors can be expressed using the MouSensor genetic platform

Authors

Charlotte D'Hulst, Raena B. Mina, Zachary Gershon, ..., Matthew E. Rogers, Yevgeniy Sirotin, Paul Feinstein

Correspondence

feinstein@genectr.hunter.cuny.edu

In Brief

D'Hulst et al. have increased the total number of neurons expressing specific mouse or human odorant receptors (ORs) in the nose of a mouse by genetically controlling OR gene choice. These MouSensors show lower specific odor detection thresholds and provide a platform to study OR gene expression and odor coding in vivo.

D'Hulst et al., 2016, Cell Reports *16*, 1115–1125
July 26, 2016 © 2016 The Authors.
http://dx.doi.org/10.1016/j.celrep.2016.06.047

CellPress

Cell Reports
Resource

OPEN ACCESS
CellPress

MouSensor: A Versatile Genetic Platform to Create Super Sniffer Mice for Studying Human Odor Coding

Charlotte D'Hulst,[1,2] Raena B. Mina,[1,2] Zachary Gershon,[1,2] Sophie Jamet,[1,2] Antonio Cerullo,[1,2] Delia Tomoiaga,[1,2] Li Bai,[3] Leonardo Belluscio,[3] Matthew E. Rogers,[4] Yevgeniy Sirotin,[5] and Paul Feinstein[1,2,*]
[1]Department of Biological Sciences, Hunter College
[2]The Graduate Center Biochemistry, Biology and Biopsychology and Behavioral Neuroscience Programs
City University of New York, New York, NY 10065, USA
[3]Developmental Neural Plasticity Section, National Institute of Neurological Disorders and Stroke, NIH, Bethesda, MD 20892, USA
[4]Corporate Research and Development, Firmenich Inc., Plainsboro, NJ 08536, USA
[5]Shelby White and Leon Levy Center for Neurobiology and Behavior, The Rockefeller University, New York, NY 10065, USA
*Correspondence: feinstein@genectr.hunter.cuny.edu
http://dx.doi.org/10.1016/j.celrep.2016.06.047

SUMMARY

Typically, ~0.1% of the total number of olfactory sensory neurons (OSNs) in the main olfactory epithelium express the same odorant receptor (OR) in a singular fashion and their axons coalesce into homotypic glomeruli in the olfactory bulb. Here, we have dramatically increased the total number of OSNs expressing specific cloned OR coding sequences by multimerizing a 21-bp sequence encompassing the predicted homeodomain binding site sequence, TAATGA, known to be essential in OR gene choice. Singular gene choice is maintained in these "MouSensors." In vivo synaptopHluorin imaging of odor-induced responses by known M71 ligands shows functional glomerular activation in an M71 MouSensor. Moreover, a behavioral avoidance task demonstrates that specific odor detection thresholds are significantly decreased in multiple transgenic lines, expressing mouse or human ORs. We have developed a versatile platform to study gene choice and axon identity, to create biosensors with great translational potential, and to finally decode human olfaction.

INTRODUCTION

Odorant receptor (OR) genes form the largest multigene family in mammals, with about 1,200 members in the mouse and 350 in humans (Zhang and Firestein, 2002). The main olfactory epithelium (MOE) expresses ORs through a poorly understood singular gene choice mechanism, whereby only one allele of any OR gene is selected for specific expression in a given neuron (Chess et al., 1994; Strotmann et al., 2000). Axons from olfactory sensory neurons (OSNs) that express identical ORs coalesce into 2 out of the roughly 1,800 glomeruli per olfactory bulb (OB). The OR coding sequence (CDS) plays a role in the maintenance of gene choice; that is, if the OR is not capable of this maintenance, then a second OR allele is tested for functionality (Feinstein et al., 2004). Hence, deletion of an OR CDS precludes the convergence of axons into a specific glomerulus and results in OSNs choosing to express one of the other OR genes and concomitantly projecting to a variety of glomeruli in the OB. In addition, OR proteins are necessary for promoting axon guidance, axon identity, and stabilizing neurons that have chosen to express those ORs (Feinstein et al., 2004; Feinstein and Mombaerts, 2004). Finally, the OR protein needs to be targeted to the olfactory cilia where it will function in odor signal transduction.

There has been limited success in odor profiling of ORs expressed in heterologous cells in vitro. Part of this limitation is due to the inability of OR proteins to traffic to the plasma membrane. In addition, given the biological properties of the olfactory system, many OR alleles characterized in vitro may not be functional in an in vivo setting and thus could be intact pseudogenes. The major drawback, however, has been the ability to rapidly contrast how odors presented to the OR in liquid phase (in vitro) correspond to odors presented in vapor phase within their mucosal environment (in vivo). Even ex vivo patching of dendritic knobs from transgenic and gene-targeted mice suffers from an absence of vapor phase delivery of odors. Finally, the study of both OR gene choice and OR coding in vivo is hampered by the low representation of a given OR, which, on average, is only expressed in 0.1% of the total neuronal population of a wild-type mouse.

To increase specific OR representation by modulating OR gene choice, we have been characterizing OR minigenes for the past decade. We have identified highly conserved motifs in the promoter sequences of several mouse OR genes that are necessary and sufficient for singular gene choice (Rothman et al., 2005; Vassalli et al., 2011). In the case of an M71 OR minigene, a 7.5-kb DNA fragment accurately recapitulates the functionality of the gene-targeted M71 locus and imparts an expression pattern paralleling that of endogenous genes. We have previously observed the following two highly conserved sequences: a single candidate Olfactory-1/Early B Cell Factor (Olf1/EBF or O/E) binding site and two candidate-LIM homeobox 2 (Lhx2) binding sites (TAATXX or HD) within a 161-bp region. Our experiments suggested that an HD sequence is critical for regulating the probability for any OR gene to be expressed (Vassalli et al., 2011).

This is an open access article under the CC BY license (http://creativecommons.org/licenses/by/4.0/).

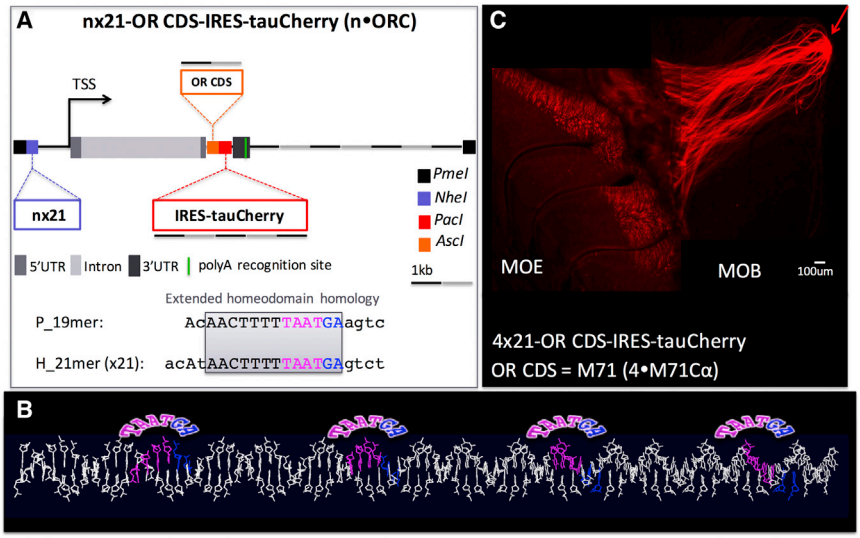

Figure 1. Transgenic Approach

(A) Design of the transgene. Top: the transgenic vector is created using the M71 OR genomic backbone. Any number of H_21-mer repeats can be shuttled in the *NheI* site upstream of the transcriptional start site (TSS), and any OR CDS can be cloned into the *AscI* site. An IRES-tauCherry cassette (*PacI*) follows the OR CDS. The internal ribosomal entry sequence (IRES) allows for bicistronic translation and simultaneous expression of mCherry, enabling the visualization of the olfactory morphology. Transgenic animals are generated by pronuclear injection of *PmeI* (black) digested DNA. Bottom: comparison of the HD binding sites in the P and H elements. A gray box highlights the extended homeodomain homology between the P and H elements.

(B) 3D rendering of the 21-mer multimerized four times. Given the fact that a DNA helix turns every 10.5 bp, multimerization of 21-mer positions the HD binding sites on the same site of the DNA, allowing for cooperative binding of transcription factors.

(C) Confocal medial whole-mount view of MOE and MOB from a proof-of-concept 4•M71Cα hemi transgenic mouse, showing the increased numbers of OSNs expressing M71 (red) and like axons projecting to a big medial glomerulus (arrow). The montage was created by merging a 5× fluorescent image of MOE and an image of its corresponding MOB.

Analysis of sequences known to strongly influence OR gene choice such as the mouse H (the homology region that activates the MOR28 cluster [Serizawa et al., 2003]) and P (a sequence with high homology to the P3 minimal promoter [Bozza et al., 2009]) elements have revealed a set of three HD binding sites (TAATGA) in close proximity to each other, and an associated O/E site, with one of the HD sites sharing the same 13-mer AACTTTT**TAATGA** between them. When a 19-mer containing this 13-mer sequence from the P element was multimerized nine times (9x19) and placed upstream of the MOR23 transgene backbone, modest increases in cell numbers were observed in 3/17 transgenic founders. Because analysis of chimeric P/P3 promoter transgenes suggested that DNA spacing of the HD might influence OR gene choice (data not shown), we designed a gene choice enhancer consisting of various multimers of a 21-bp sequence from the H element (ACATAACTTTT**TAATGA**GTCT), each covering two DNA turns of 10.5 bp and thereby allowing for maximum cooperativity of transcription factors, resulting in a radical increase in expression of any cloned OR CDS, which was never obtained with the 9x19 transgenic approach. We refer to these designer mice as "MouSensors."

We provide a genetic platform, which increases the total population of OSNs expressing a specific OR, enabling us to robustly study OR gene choice, axon identity, and odor coding simultaneously in its intact in vivo environment. Importantly, we show that we can also express human ORs in large numbers of mouse OSNs in our MouSensors, providing a breakthrough technology to crack the human olfactory code.

RESULTS

The MouSensor Transgene

Using the previously described M71 minigene (Rothman et al., 2005), we re-designed the transgenic vector in a modular way such that any number of the 21-bp enhancer sequence (ACATAACTTTT**TAATGA**GTCT) and any OR CDS of interest can be cloned (Figure 1). The addition of a bicistronic reporter allows for the visualization of the olfactory neuronal morphology.

Effect of 21-mer Multimerization on the Organization of the Olfactory System

Here we tested the effect of our newly designed enhancer element on increasing the probability of OR gene choice. We performed an initial analysis of various M71 transgenic lines containing 0, 1, 2, 3, or 4 multimers of the 21-mer sequence (Table S1). We conclude that less than 50% of germline animals containing fewer than four 21 multimers show expression of the cloned OR and none of them are robust expressers. On the contrary, all 4x21 M71 lines generate robust increased expression (3/3 germline animals); we have bred two 4x21-M71 lines (4•M71Cα and β) for further analysis.

Subsequently, we assessed whether the copy number of the transgenes insertions influences the rate of OR expression by real-time qPCR as previously described (D'Hulst et al., 2013) and found no correlation between the expression level and copy number. Hemizygous 4•M71Cα contain ~15 copies, whereas hemizygous 4•M71Cβ showed ~24 copies. Interestingly, 9 0•M71C founders contained between 5 and 32 insertions of the transgene, but do not show any robust OR expression (Tables S1 and S2). We hypothesize that our 4x21 enhancer is able to recruit factors that can modulate the chromatin environment and, as such, promotes specific OR expression when randomly inserted in the genome.

To contrast the effect of increasing choice of the M71 OR in the 4•M71Cα line on the expression level of the "endogenous" M71 OR on axon guidance and identity, we crossed this line to M71-IRES-tauGFP mice gene targeted at the M71 locus (M71-GFP, 129 strain) (Feinstein et al., 2004). This established a new mouse line that is either homozygous for M71-GFP (*M71-GFP*$^{-/-}$,

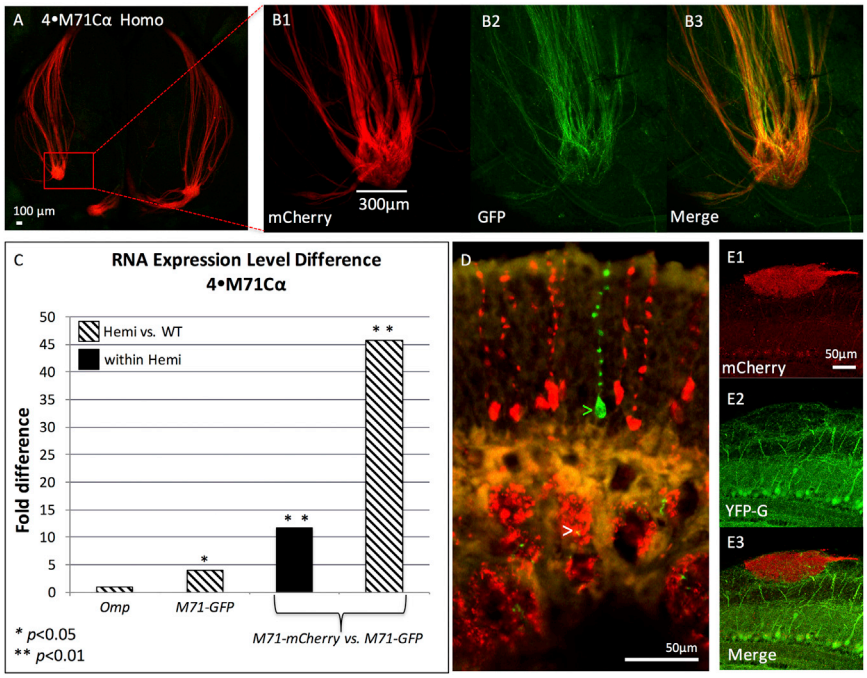

Figure 2. Molecular Characterization of the 4·M71Cα MouSensors

(A) Confocal picture of a dorsal whole-mount MOB of 4•M71Cα homo; *M71G*$^{-/-}$ showing M71 glomeruli in red.

(B) Red axons (from the M71 transgenic OSNs) and green axons (from the M71 gene-targeted OSNs) co-converge onto the same M71 glomerulus, showing intact axon guidance in the M71 MouSensors (B3, overlay).

(C) Real-time qPCR with hydrolysis probes. Left: *Omp* (encoding the olfactory marker protein, expressed in all mature OSNs) RNA levels are equally expressed between 4•M71Cα hemi and WT (0.98-fold). Endogenous RNA levels of *M71-GFP* are significantly increased 3.89-fold in the 4•M71Cα hemi line, suggesting that increasing the probability of choice of M71-mCherry affects the endogenous RNA levels of *M71* as well. The level of *M71-mCherry* RNA is significantly increased by ~12-fold when compared to *M71-GFP* levels within the 4•M71Cα hemi line and by ~45-fold when compared to *M71-GFP* levels in the WT.

(D) Coronal cryosection (25×) of the MOE of a 4•M71Cα hemi animal showing conserved monoallelic expression, i.e., red and green cells never co-express. M71-GFP positive OSNs and axons are indicated with a green and white arrow, respectively.

(E) Confocal images of OB tissue (cryosectioned coronally) of F1 offspring of a cross between our 4•M71Cα hemi and YFP-g mice (JAX Mice Database, strain: 014130) showing normal mitral cell innervation (green, E2) of the M71 transgenic glomerulus (red, E3).

henceforth known as WT) or homozygous for M71-GFP and hemizygous or homozygous for the M71-IREStauCherry transgene (*4•M71Cα*$^{+/0}$*;M71-GFP*$^{-/-}$ or *4•M71Cα*$^{+/+}$*;M71-GFP*$^{-/-}$ henceforth known as 4•M71Cα hemi or homo, respectively). In our 4•M71Cα line, the increase of OSNs expressing the M71 OR results in the coalescence of labeled axons onto one lateral glomerulus and one medial glomerulus per OB side (Figure 2), which are significantly larger (calculated spherical radius of 80–100 µm) than typical glomeruli (radius of ~33 µm [Bressel et al., 2016]). We confirmed the linear correlation between the number of OSNs expressing a given OR and the total volume of corresponding glomeruli in the OB, by performing real-time qPCR to quantify M71 OR expression in the MOE (Figure 2; Tables S4 and S5). We find that the level of *M71-Cherry* RNA is significantly increased by ~12-fold ($p < 0.01$) when compared to *M71-GFP* within the hemi 4•M71Cα line and by ~45-fold ($p < 0.01$) when compared to *M71-GFP* in the WT line. This apparent discrepancy is explained by the fact that the expression of the gene-targeted *M71-GFP* is 3.89-fold higher in the 4•M71Cα hemi animals when compared to the WT animals ($p < 0.01$). These numbers suggest that increasing *M71-Cherry* RNA levels help stabilize the endogenous *M71-GFP* RNA levels early in development in the 4•M71Cα line, instead of cannibalizing their ability to be chosen, leading to an increase in endogenous M71 transcripts in the 4•M71Cα animals. This model is supported by the fact that OSNs are interdependent in maintaining axonal projections (Ebrahimi and Chess, 2000). Importantly, we show that we have not changed the total number of mature OSNs in the 4•M71Cα animals (real-time qPCR shows that olfactory marker protein [*omp*] RNA levels are not changed between 4•M71Cα and WT animals [Figure 2]). This real-time qPCR analysis together with calculations of the total glomerular volume (TGV) using 4•M71Cα MOE sections (data not shown) allow us to estimate the total increase in M71 OR expression in 8-week-old hemi 4•M71Cα animals to about 1% of the total OSN population as compared to 0.02% in WT animals, assuming a total of 10 million total OSNs (Bressel et al., 2016).

Finally, because glomerulus-like structures may form in absence of postsynaptic olfactory neurons (Bulfone et al., 1998), we assessed whether the postsynaptic bulbar circuitry necessary to convey olfactory sensory information to the higher cortical regions remains intact (Belluscio et al., 2002). Therefore, we crossed an existing YFP-g transgenic mouse line (in which 30% of the postsynaptic mitral cells are labeled in yellow) to the 4•M71Cα line to visualize mitral cell dendrites (Figures 2 and S1). We establish that mitral cell innervation of the M71 glomerulus appears to be unchanged, as dendrites from postsynaptic mitral and tufted cells are present.

Singular Gene Expression in the 4·M71Cα Line

Monogenic and monoallelic expression of OR genes is a prerequisite for proper function of the olfactory system. Therefore, we assessed whether this mechanism of singular gene choice is maintained in our 4•M71Cα MouSensors.

Using coronal cryosections of the MOE of 4•M71Cα hemi animals, we have counted a total of 4,754 Cherry-positive cells expressing the M71 4x21 transgene and 221 GFP-positive cells expressing the M71-GFP gene-targeted mutation; none of the red cells co-express the green marker in the MOE, suggesting that the 4x21 M71 transgene maintains monogenic expression

(Figure 2). In addition, confocal imaging of the OB of these animals reveals co-convergence of Cherry-positive and endogenous GFP-positive axons onto the same isotypic M71 glomerulus (Figure 2), showing that OSNs expressing the M71 transgene have the same axonal identity as endogenous M71 OSNs (represented by the GFP-tagged mutation). Axonal identity strictly correlates with the most abundant OR expressed in an OSN (Bozza et al., 2002), thus it is unlikely that other ORs are enriched in 4•M71Cα OSNs. Moreover, it is improbable that the level of M71 RNA transcripts is elevated in the 4•M71Cα OSNs as they coalesce with M71-GFP axons; this is consistent with our previous observations that axons of OSNs expressing MOR23 from the 9x19 transgene co-converge into the same glomeruli as axons of OSNs expressing MOR23 from the endogenous locus (Vassalli et al., 2011) and our acute awareness that subtle changes to OR levels have dramatic effects on axon identity (Zhang et al., 2012).

In Vivo SynaptopHluorin Imaging of Glomerular Activity

Our MouSensor approach provides us with the opportunity to answer a long-standing question in the field of olfaction: What is the effect of increasing axonal input to a single glomerulus on odor responses and behavior?

Because the M71 OR is dorsally expressed in the OB, any cloned OR using the M71 transgenic backbone will coalesce its axons onto dorsally located glomeruli, which makes them accessible for optical imaging. To functionally examine the transgenic M71 projections in the OB, we imaged odor-evoked activity from the OBs of mice expressing the genetically encoded activity reporter synaptopHluorin (SpH) in all mature OSNs (Bozza et al., 2004). We recorded from mice that were either hemi or homo for 4•M71Cα (gene-targeted M71-GFP is out crossed) and heterozygous for SpH and identified the fluorescent glomeruli by thinning the bone overlying the OB. We used nine different M71-selective ligands from ex vivo analysis of genetically defined M71 OSNs in gene-targeted mice (Zhang et al., 2012): three of these ligands produced robust responses by SpH imaging: Acetophenone (ACP), 4-Methylacetophenone (4MACP), and 2,4-Dimethylacetophenone (24dMACP) when delivered at different odor dilutions (in nitrogen [N_2]) varying between 0% and 15% (Figures 3 and S2).

M71 Ligands Show the Same Efficacy but Different Apparent Affinity in Hemizygous 4·M71Cα Animals

In 4•M71Cα hemi animals, the average highest $(dF/F)_{max}$ is 3.63% for ACP (n = 7 glomeruli at 1.33 μM), 4.48% for 4MACP (n = 9 at 0.69 μM), and 4.15% for 24dMACP (n = 7 at 0.66 μM). These results show that all three compounds cause a similar efficacy (i.e., average $(dF/F)_{max}$: maximum response obtained by a compound) in terms of M71 OR activation (a one-way ANOVA comparing the highest $(dF/F)_{max}$ values between hemi animals did not reveal any significant differences). However, the apparent affinity of the M71 OR for 4MACP and 24dMACP is significantly higher than ACP since the latter two compounds start activating the M71 glomerulus at a lower concentration (Figures 4 and S2, triangles). For example, when delivered at the same concentration (i.e., ~0.70 μM), efficacy for ACP (0.73%, n = 4) is significantly lower than the efficacy for both 4MACP (4.48%, n = 9, $p < 0.0001$) and 24dMACP (4.15%, n = 7, $p < 0.0001$). Hence, similar odor efficacy is observed at lower concentrations for both 4MACP and 24dMACP when compared to ACP responses in the hemi animals (Figures 4 and S2).

Increasing the Number of OSNs Expressing M71 Changes the Efficacy for Both High- and Low-Affinity Ligands

In 4•M71Cα homo animals, the highest efficacy for ACP is 4.57% (n = 14 at 2.66 μM), 3.82% for 4MACP (n = 16 at 0.69 μM), and 4.92% for 24dMACP (n = 7 at 0.44 uμM). To assess the influence of both *genotype* and *concentration* on the $(dF/F)_{max}$, we performed a two-way ANOVA statistical analysis for each odor dataset. For all odors tested, we see a significant effect of the concentration on the response; ACP: $p = 0.0002$, 4MACP: $p = 0.0003$, and 24dMACP: $p < 0.0001$. For ACP and 24dMACP, we also see a significant effect of the genotype on the response, i.e., ACP: $p = 0.008$ and 24dMACP: $p = 0.0018$. However, the interaction between genotype and concentration is not significantly different for both odors. This observation can be explained by the fact that we only see significant differences between hemi and homo at specific concentrations of both ACP and 24dMACP and not at all concentrations tested (Figure 4, boxed). Indeed, when ACP is delivered at 0.71 μM in the homo group, the efficacy is 3.00% (n = 6), which is significantly higher ($p < 0.05$) than the response at the same concentration in the hemi group (0.73%, n = 4), reflecting a change in apparent affinity for this ligand when increasing the number of M71 expressing neurons. Moreover, at the highest ACP concentration we delivered (i.e., 2.66 μM), the homo response is also significantly higher than the hemi response (4.57%, n = 14 versus 3.46%, n = 9, $p < 0.05$). For 24dMACP, we see a significant increase in efficacy at 0.44 μM (4.92% [n = 7] versus 2.92% [n = 4], $p < 0.01$) when comparing the homo and the hemi group. In addition, the average efficacy (of all concentrations and odors) is significantly different between 24dMACP and 4MACP in homozygous animals (4.92% versus 3.83%, $p = 0.0272$), even though they show practically the same dose response in the hemi group (Figures 4 and S2). Thus, further increasing the number of neurons (from hemi to homo) expressing the M71 OR changes the efficacy of 24dMACP, empirically identifying it as the higher-affinity ligand.

In conclusion, given a defined number of OSNs expressing M71, saturation of the glomerular response is reached at certain concentrations of a given odor. However, this saturation response is not determined by a specific subset of OSNs expressing one OR type. In our study, the use of an in vivo anesthetized preparation using SpH imaging is sufficient to support our observation that 4•M71Cα glomeruli are functional and that more neurons increase glomerular response. There are no published studies that systematically examine the effects of anesthetics on SpH imaging, which is likely a more accurate representation of OSN response since its signals are clearly based on synaptic vesicle fusion while the signals for intrinsic signal imaging are a bit more ambiguous. It is unlikely that unstable anesthesia is the basis for the observed changes in glomerular activation, but rather it is more likely a consequence of interglomerular circuitry, which has been shown to exhibit lateral effects on glomeruli within the region (Wilson and Mainen, 2006). Since

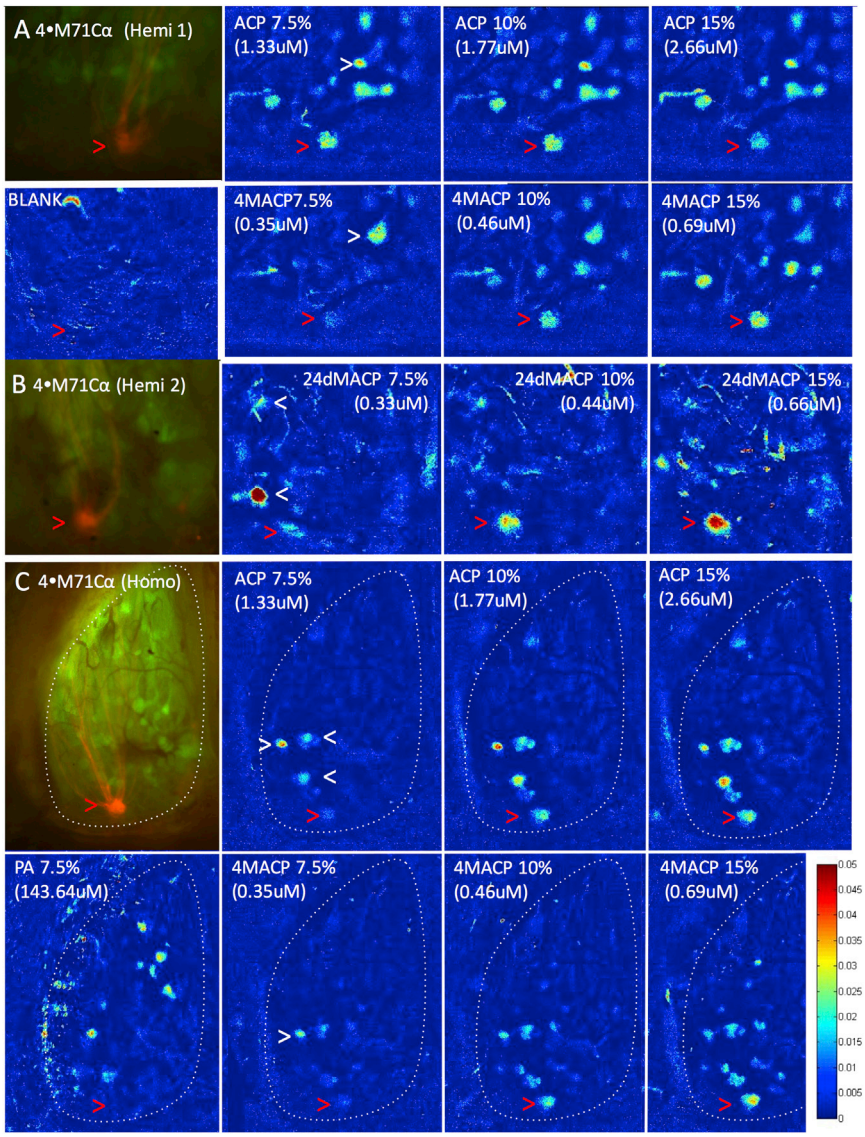

Figure 3. In Vivo SynaptopHluorin Imaging: M71 Transgenic Glomerulus Is Activated by Known M71 Ligands

Green panels show the resting SpH fluorescence imaged through dorsally thinned bone (M71 glomerulus shown in red). Pseudocolored panels show the mean dF/F (%) response during the odor stimulus period (4 s). Anterior is up.

(A) Right bulbar area of a 4•M71Cα hemi mouse showing activation of the M71 glomerulus (red arrow) and recruitment of other glomeruli upon presentation of different concentrations (7.5%–15%) of ACP and 4MACP. Note the difference in actual delivered vapor concentration (at the same odor dilution) between the odors due to their different saturated vapor pressures (Table S3).

(B) Left bulbar area of a 4•M71Cα mouse (hemi 2) showing glomerular activation by 24dMACP. M71 glomerulus is indicated with red arrow. A blank trial (0%) is shown on the top left.

(C) Glomerular activation by ACP and 4MACP of a homozygous 4•M71Cα mouse. The dotted lines demarcate the edges of the left olfactory bulb. Both ACP and 4MACP activate the Class II domain of the dorsal bulb (including the red M71 glomerulus). Left bottom panel shows glomerular activation by propyl acetate (PA, 7.5%), indicating that our 4•M71Cα mouse line is still able to detect "non-M71 ligands" as well.

(A–C) Responses are not confined to the M71 glomerulus alone. White arrows show other glomeruli that are more strongly activated than the M71 glomerulus (red arrow), by low concentrations (7.5%) of ACP (1.33 μM), 4MACP (0.35 μM), and 24dMACP (0.33 μM), suggestive of the existence of ORs with higher affinity for all odors tested.

SpH imaging reflects only the activity of OSNs, the lateral inhibition from neighboring glomeruli associated with changes in odor concentration may produce a sudden decrease in fluorescence in some glomeruli while others become active. By contrast, experiments in awake-behaving animals are highly susceptible to a variety of top-down signals from higher brain regions (Blauvelt et al., 2013). These centrifugal signals originate from various brain regions and can clearly modify the odor response (Liu et al., 2015; Rothermel et al., 2014), which in turn alters or could potentially mask different aspects of the pure OSN odorant evoked signal, which we are testing here.

Ex Vivo versus In Vivo Ligand Profiling

In our setup, odors are delivered from the headspace of odor saturator vials containing 99% pure odorants and flow-diluted with air (N_2) prior to delivery to the anesthetized animal. The molar vapor concentration (μM) reaching the animal's nose is therefore determined by odorant-saturated vapor pressure (*P*s), which can differ dramatically between odorants. For example, 15% air dilution of ACP (*P*s = 0.3260 mmHg at 25°C) generates 2.66 μM concentration in air, while 4MACP and 24dMACP (*P*s = 0.0849 and 0.0811, respectively) are delivered at 0.69 μM and 0.66 μM, respectively (Table S3). We compared in vivo responses with previous ex vivo data (Zhang et al., 2012), by initially analyzing nine different odors that did (Benzaldehyde [BA], Ethylmalthol [EM], 2-Amino-acetophenone [2AACP], ACP, 4-Metoxyacetophenone [4MOHACP], 4MACP, and 24dMACP) or did not (Methylbenzoate [MB] and Menthone [M]) elicit an M71 response through ex vivo patch clamping of dendritic knobs when delivered in liquid phase. We only observed glomerular activity with ACP, 4MACP, and 24dMACP. There are two reasons for these findings: the odor is not delivered at a high enough concentration and/or the odor may not generate a high enough activation within OSNs. We find that the minimal *P*s necessary to be able to elicit a response in vivo is 0.0811 mmHg (which is the *P*s of 24dMACP; Figure S3). 4MOHACP (a high responder ex vivo; *P*s = 0.0133 [< 0.0811] mmHg) and BA (a low responder ex vivo that has the highest

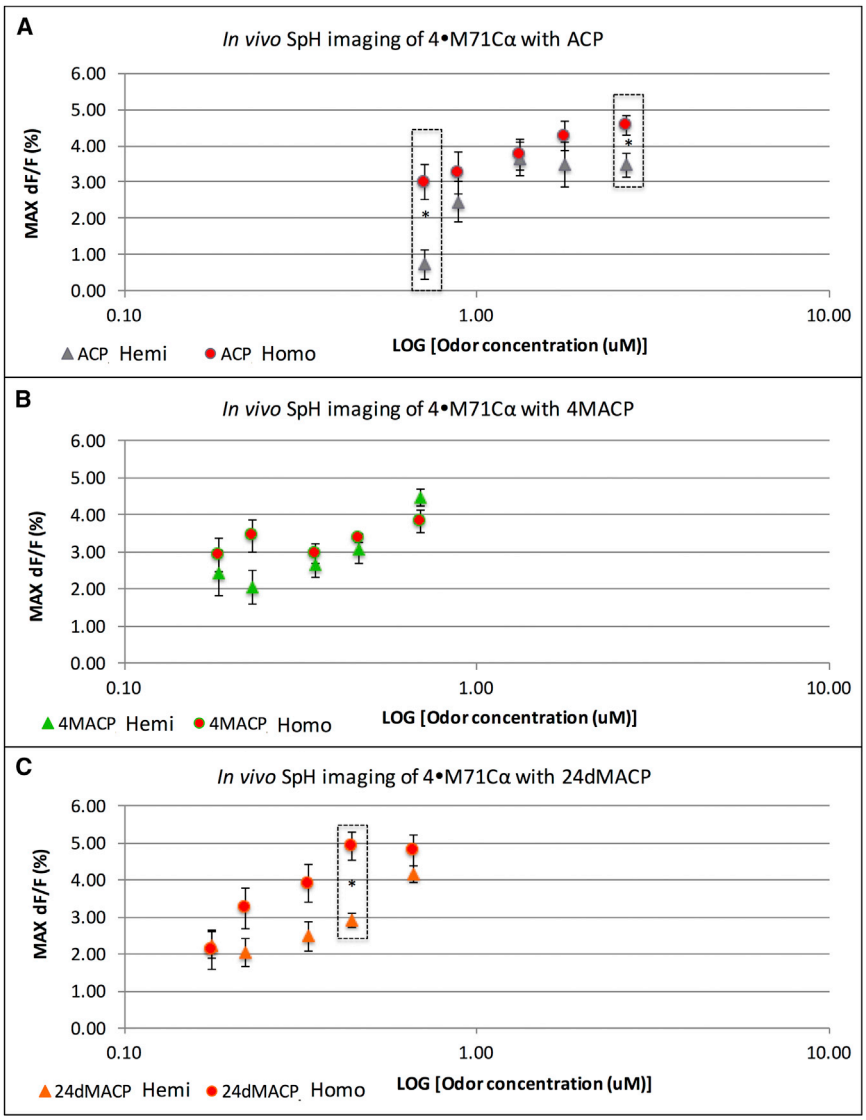

Figure 4. Individual Odor Response Profiles of In Vivo Glomerular Imaging of M71 MouSensors: 4·M71Cα

(A–C) Responses for ACP (gray; A), 4MACP (green; B), and 24dMACP (orange; C). The odor concentration, presented as the calculated vapor concentration (μM), is indicated on the log x axis. The average max dF/F (%) is indicated on the y axis. Each data point represents the average $(dF/F)_{max}$ for 4–16 glomeruli. Error bars represent the SEM. Triangles indicate responses from hemizygous animals, and red circles indicate homozygous animals. Asterisks indicate homozygous responses that are significantly higher than hemizygous responses when the animals are presented with the same odor concentration (using a Student's t test). All imaged mice are heterozygous for *omp-SpH*.

*P*s of all odors tested; = 1.0100 mmHg at 25°; Figure S3) do not show glomerular activation in vivo. Hence, we suggest that when the minimal *P*s requirement is met, a minimum current amplitude (pA) M71 response (ex vivo) is necessary for an odor to activate M71 glomeruli in our SpH imaging setup; this is the so-called "sweet spot" for generating an in vivo response (black dashed line in Figure S3). To further test this hypothesis, we imaged one additional 4·M71Cα hemi animal with two extra M71 ligands (i.e., Propiophenone [PP] and 2-Hydroxyacetophenone [2OHACP]; Figure S3) that generate similar responses ex vivo when delivered in liquid, but have a different *P*s (PP: 0.149000 and 2OHACP: 0.07020, respectively); only 2OHACP elicited a response in our hands (data not shown), even though it has a lower *P*s. This suggests that 2OHACP is a better ligand, which reinforces our point that the *P*s must be considered when assessing the strength of a ligand; thus, the best in vivo odors will have the combination of maximum ex vivo responses and lowest *P*s value. For the M71 OR, it is 24dMACP.

Odor Detection Threshold in a Two-Bottle Discrimination Behavioral Task

Sensitivity studies performed in Wistar neonate and adult rats have shown that the highest sensitivity to an odor (lowest threshold) correlates with the highest OSN density in the MOE (Kraemer and Apfelbach, 2004). Therefore, we assessed whether detection of the most robust M71 ligand is amplified in our 4·M71Cα MouSensor line. We use an avoidance task in which the odorant 24dMACP is added to drinking water and becomes an aversive stimulus associated with injection of lithium chloride (LiCl), a compound known to induce gastric malaise (Cheng et al., 2013). We chose to use 24dMACP because SpH imaging with this odor produced the greatest responses of any odor tested at low concentrations and this level could be altered with increasing numbers of M71 expressing neurons. After conditioning homo 4·M71Cα animals and their WT littermates to water containing a 10^{-4} dilution of 24dMACP, the animals are given the choice between plain water and water with decreasing concentrations of 24dMACP (10^{-4}, 10^{-6}, 5×10^{-7}, and 10^{-7}). Note that all tested animals are homozygous for M71-GFP, so even WT ones have a functional M71 OR.

The results are presented as a preference index (PI) for the odorized water for each group of animals, which is calculated as the amount of the odorized water consumed divided by the total amount of liquid (odor and no-odor water) consumed over a 24-hr time period (Figure 5A). A PI of 50% reflects no preference of the animal. After conditioning, both WT and 4·M71Cα homo animals show a clear aversion toward 10^{-4} and 10^{-6} dilutions of 24dMACP reflected through an average PI for 24dMACP. However, when 24dMACP is delivered at 10^{-7}, all animals fail to detect the presence of the odor with an average PI of 45.38% for the WT (n = 8) and 58.76% for the homozygous

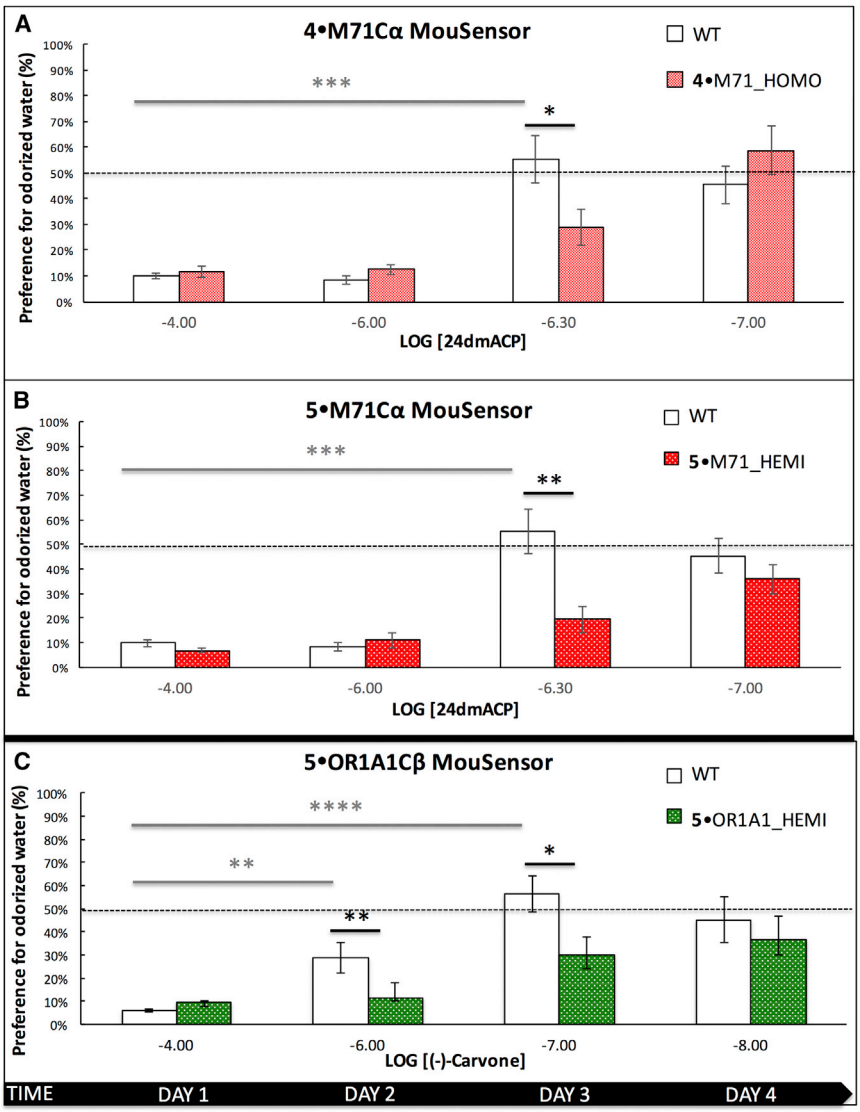

Figure 5. Behavioral Avoidance Assay Using a Two-Bottle Odor Discrimination Task to Test Enhanced Sensitivity of Specific MouSensors

The ratio of the odorized solution consumed to the total solution consumed expressed as a percentage (preference index [PI]) is shown on the y axis and represents the preference of the animals for water containing the odor. A dotted horizontal line indicates a PI of 50%, where animals do not have a preference for either odor presented. Error bars represent the SEM. The x axis shows the dilution of the odorized solution on a logarithmic scale. The black arrow indicates the time; mice were trained for several days starting at highest odor concentration and then were given the choice between drinking from a non-odorized solution or a solution containing the odor in the "training" dilution, which is the day 1 time point. Subsequently, every 24 hr (days 2, 3, and 4) the concentration of the odorized solution was lowered, respectively, until no preference was observed between drinking either solution.

(A) 4•M71Cα MouSensor. Comparison of 4•M71Cα homo (n = 8) with WT controls (n = 8) in detecting the high-affinity M71 ligand, 24dMACP. Homo animals show a 0.3-log decrease in detection threshold (*t test)

(B) 5•M71Cα MouSensor. Comparison of 5•M71Cα hemi (n = 9) with WT controls (n = 8) in detecting the high-affinity M71 ligand, 24dMACP. Hemi animals show a 0.3-log decrease in detection threshold (*t test).

(C) 5•OR1A1Cβ MouSensor. Comparison of 5•OR1A1Cβ hemi (n = 12) with their WT littermates (n = 7) in detecting the high-affinity OR1A1 ligand (−)-Carvone. Hemi animals show a 2-log decrease in detection threshold for the 5•OR1A1Cβ MouSensor (*t test).

animals (n = 8). This suggested that if the sensitivity of these M71 MouSensors were changed, the threshold would be between 10^{-6} and 10^{-7}. Indeed, the PI of the WT group is significantly higher than the PI of the mutants at dilution 5×10^{-7} (55.32% versus 28.83%, $p < 0.05$), showing that while the WT fail to detect the odor at 5×10^{-7}, the MouSensors still show aversion behavior and thus still smell 24dMACP. Importantly, the WT animals also show a lower PI for the odorized water at 10^{-4} than at 5×10^{-7} (9.88% versus 55.32%, $p < 0.001$), indicating that the behavioral difference is most likely a result of the increased ability of the MouSensors to detect the odor rather than a learning deficiency in the WT (Figure 5A, gray bars). As a reference, a 10^{-6} dilution of 24dMACP corresponds to 6.46 μM, a concentration that can be easily detected by both homo and WT animals and does not cause an aversive response by itself (the PIs for drinking water containing 10^{-6} of 24dMACP for naive, unconditioned mice are as follows: WT: 60% ± 7.72 [n = 5] and homo: 59%. ± 1.94 [n = 5]). In our imaging studies, non-M71 glomeruli could respond to ACP, 24dMACP, and 4MACP; however, response rates for 24dMACP were more robust for M71 and did not easily desensitize, suggesting that for a given ligand-OR pair, behavioral differences can be observed.

M71 MouSensors Do Not Have a Monoclonal Nose

Given the fact that the 4•M71Cα MouSensor animals express the M71 OR in ~1%–2% of the their OSNs, our transgenic M71 line is different from the animals generated by Fleischmann et al. (2008), where the neural representation of odors was altered significantly by decreasing expression of most ORs by 95% and replacing them with M71, creating animals with a monoclonal nose. Despite their observation that ACP (weakly) activated most OSNs and glomeruli, odor discrimination and performance in associative learning tasks is impaired in these animals. One possible explanation for this behavior is that broad uniform activation (such as in the monoclonal nose) may cause lateral inhibition through intricate feedback mechanisms (at the level of detection and/or perception) and ACP may be detected as olfactory "noise." In this regard, many small glomeruli could

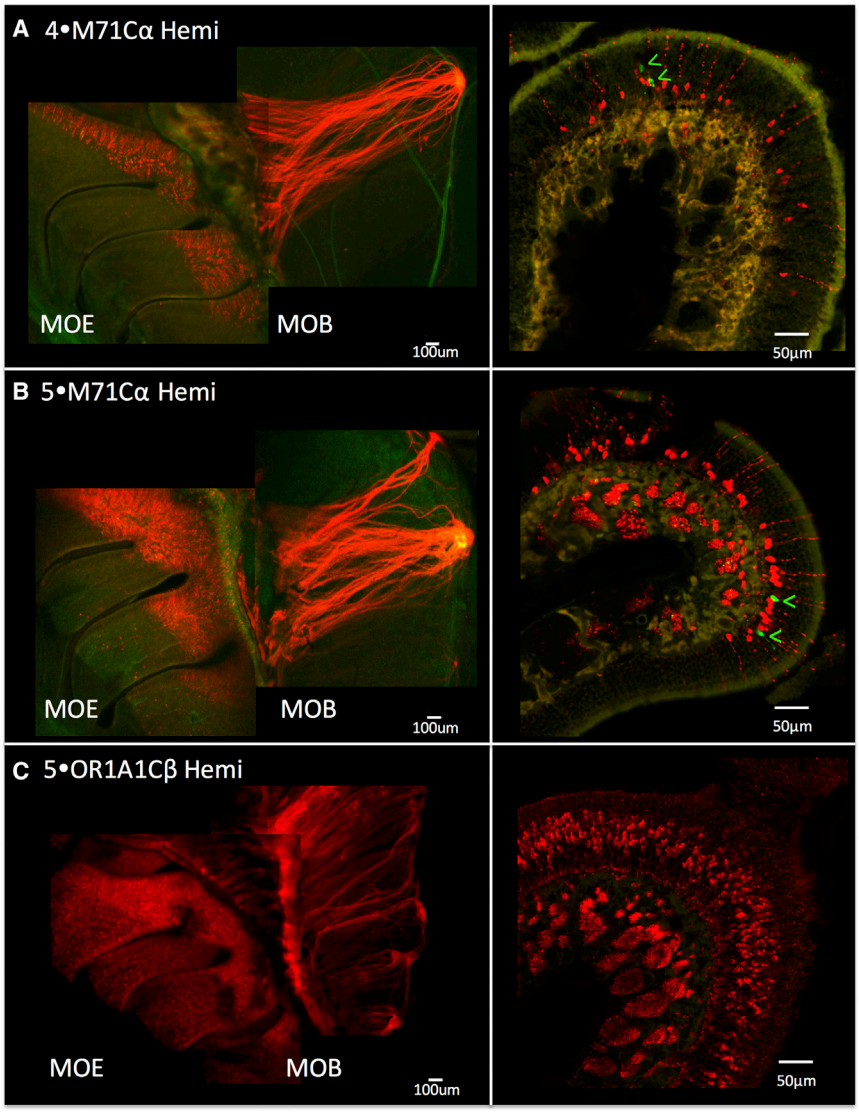

Figure 6. Versatility of the MouSensor Platform

Left: confocal images of the medial whole-mount view of the MOE with OSNs projecting their axons to glomeruli in the MOB. Each montage was created by merging a 5× fluorescent image of MOE and an image of its corresponding MOB. Right: coronal cryosections of the MOE. OSNs expressing the transgenic M71 OR are labeled in red.

(A) 4•M71Cα hemi; $M71G^{-/-}$ (p25).

(B) 5•M71Cα hemi; $M71G^{-/-}$ (p27). Red OSNs are abundantly present in the MOE, and their axons co-converge onto glomeruli that are not confined anymore to the dorsal zone.

(C) 5•OR1A1Cβ hemi mouse (p31). Red OR1A1 axons are abundantly present in the MOE, and several stable glomeruli are formed in the OB (see Figure S5B). Since OR1A1 is a human OR, we cannot gene target the endogenous gene for OR1A1 in the mouse with a GFP reporter to compare expression levels (like we did for the M71 MouSensor), hence the absence of green in the bottom panels.

be disadvantageous compared to fewer very large glomeruli (which are observed in our 4•M71Cα line) and patterned activation may be necessary for signal detection. On the other hand, by reducing the representation of endogenous OR genes by 20-fold, they may have ablated the high-affinity OR for ACP as well (e.g., Olfr145; von der Weid et al., 2015). The latter explanation is supported by the fact that we, and others (Zhang et al., 2012), have shown that ACP is not the best ligand for M71. In support of this notion, Nguyen and Ryba (2012) showed that overrepresentation of the I7 OR in mice does increase their sensitivity to a high affinity odor, octanal.

MouSensor: A Versatile Platform

To assess the effect of further increasing the number of multimers as a ubiquitous enhancer on the number of OSNs choosing to express any cloned OR, we additionally created MouSensors containing five 21-mers for two mouse ORs, M71, and MOR122-2. All founders for 5•M71C (6/6) and one germline animal, 5•M71Cα, show high levels of M71 expression (Table S1) and form glomeruli in the bulb (Figures 6B and S4). In addition, all five germline animals for 5•MOR122-2 show high levels of expression for MOR122-2, three of which are shown in Figure S5. Based on our TGV calculations using 5•M71Cα sections (Bressel et al., 2016), we find that adding an extra 21-mer to the M71 MouSensor transgene increases the number of OSNs expressing the M71 by 1.5-fold to about 1.6% of the total OSN population in hemi animals (Figures 6A and 6B). Importantly, this increased number appears to be a result of multimerization and not of increased copy number of the transgene in the genome (~16 times for 5x21 M71 versus ~15 for the 4x21 M71 transgene; Table S2). In addition, using 35 coronal cryosections from the MOE of 6.5-week-old 5•M71C hemi animals, we did not observe any coexpression of 52 green cells among a large population of red cells (too numerous to get an accurate count; Figure 6B). These data show that adding five 21-mers maintains singular gene expression in OSNs. Based on current models of singular gene choice, this choice enhancer can still be suppressed in a large number of neurons and should be a target of silencing in non-cherry cells. We now have a model system for testing the role of CDSs or other genomic sequences for its capacity to be silenced (Magklara et al., 2011).

To compare specific odorant sensitivity between the 5•M71Cα and the 4•M71Cα line, we performed the two-bottle discrimination behavioral task with 24dMACP as described above (Figure 5B). In summary, we find that at dilution 5×10^{-7} the average PI of the 5•M71Cα group ($n = 9$) is 19.62%, which is significantly ($p < 0.01$) lower than the PI of the WT group ($n = 8$; 55.32%). Even

though we observe the same but slightly more significant 0.3-log decrease in odorant detection threshold in the 5•M71Cα line, it is important to mention that we used 5•M71Cα hemi animals, which have ~1.6% of their OSNs expressing M71 (similar to the 4•M71Cα homo animals with ~2% M71 expressing OSNs).

It is important to note that we are not performing precise odor-thresholding based on number of OSNs. However, it would be interesting to develop a series of M71 neuronal representations and determine how their glomerular responses and behavioral changes correlate. In addition, it is unlikely that our results are due to increased OSN responses from associative learning as the vast excess of M71 OSNs far outnumbers any change previously observed from this learning paradigm (Kass et al., 2013).

Decode Human Olfaction

To further evaluate the versatility of this platform, we have cloned a human OR using the 5x21 M71 transgenic backbone and successfully increased the probability of choice of expression of OR1A1. Both germline animals (5•OR1A1C β and δ) show robust expression of the human OR1A1 receptor in the MOE and stable glomerular formation in the OB (one of which is shown in Figures 6C and S5). Real-time qPCR reveals a ~12-fold increase of *OR1A1* RNA in the 5•OR1A1Cβ hemi animals when compared to the *M71* RNA levels in the 4•M71Cα hemi line, which translates into an estimated total of ~13% of OSNs expressing this OR (assuming a total of 10 million OSNs in 8-week-old animals). Again, *omp* levels were not changed. Clearly, the representation of some ORs must be decreased to explain this equilibrium (Serizawa et al., 2003). As was observed with the 4•M71Cα line, we find that monoallelic expression remains intact even in a MouSensor line containing large numbers of OSNs expressing OR1A1, by crossing the 5•OR1A1Cβ to the M71-GFP line. None of the red axons (expressing OR1A1) coalesce onto green glomeruli (expressing M71); instead both ORs project their axons to distinct glomeruli (Figure S6). In addition, in vivo SpH imaging (data not shown) of the OR1A1Cβ line also shows functional glomerular activation with its known ligand (−)-Carvone (Saito et al., 2009).

In the 4•M71Cα homo animals and 5•M71Cα hemi animals, a mere 2-log increase in M71 expressing OSNs leads to a significant 0.3-log change in threshold. Therefore, we hypothesize that further increasing the neuronal representation of specific ORs may decrease detection thresholds even more. We have tested this hypothesis using our established two-bottle behavioral avoidance task with the 5•OR1A1Cβ MouSensors (Figure 5C). We conditioned 5•OR1A1Cβ hemi animals (n = 12) and their (WT) non-transgenic littermates (n = 7) to water containing a 10^{-4} dilution of (−)-Carvone. For 4 consecutive days, animals were given the choice between plain water and water with decreasing (10^{-4}, 10^{-6}, 10^{-7}, and 10^{-8}) dilutions of (−)-Carvone (Figure 5C). Both groups (WT and hemi) show clear aversion toward a 10^{-4} dilution of (−)-Carvone (average PI WT = 6.17% and average PI hemi = 10.26%), reflecting successful conditioning. Both WT (average PI = 55.52%) and hemi (average PI = 47.88%) cannot detect a 10^{-8} dilution of (−)-Carvone. At 10^{-6} and 10^{-7}, however, there is a clear difference in detection between WT and hemi (10^{-6}: average PI WT = 27.65% versus average PI hemi = 11.38, $p < 0.01$ and 10^{-7}: average PI WT = 53.88% versus average PI hemi = 30.24, $p < 0.05$). These findings indicate that expressing OR1A1 in about 13% of the OSNs translates into a 2-log decrease in (−)-Carvone detection thresholds. However, a delicate balance must exist between cell number and sensitivity (Fleischmann et al., 2008). Again, the WT animals show significantly lower PIs for the odorized water at 10^{-4} than at 10^{-6} (6.17% versus 27.65%, $p < 0.01$) and at 10^{-7} (6.17% versus 53.88%, $p < 0.0001$), indicating that the behavioral difference is most likely a result of the increased ability of the mutants to detect the odor rather than a learning deficiency in the WT (Figure 5C). In addition, we find that 5•OR1A1Cβ hemi and WT (n = 5 for both groups) do not show detection threshold differences toward a non-OR1A1 ligand after being conditioned toward 24dMACP (data not shown), which proves that the effect we observe is ligand-specific.

Conclusions

We observe that placing specific HD elements in close proximity to OR genes favors dramatically increasing the probability that OR promoters are chosen. It has not escaped our attention that the MouSensor transgenic platform is an invaluable tool to further study and refine the mechanisms of singular gene choice and axonal identity. Being able to generate any OR MouSensor opens up an array of translational applications as well. We have produced biosensors with an enhanced inherent sense of smell, which can be applied to address global health and safety challenges such as identification of explosives, contraband searches, and odor-based disease diagnosis (He et al., 2015). Moreover, training of these MouSensors, or for that matter, Rat or DogSensors, in odor-detection tasks will be significantly shorter and more efficient because of the selective amplification of detection for a given subset of odors. In addition, the possibility to express human ORs in large numbers of mouse OSNs using the MouSensor technology provides a breakthrough in vivo approach to finally crack the olfactory code.

EXPERIMENTAL PROCEDURES

Subjects

Mice used in this study were bred and maintained in the Laboratory Animal Facility of Hunter College, CUNY. The Hunter College IACUC approved all procedures. Animal care and procedures were in accordance with the Guide for the Care and Use of Laboratory Animals (NHHS Publication No. [NIH] 85-23). The omp-synaptopHluorin mice were a kind gift from Dr. Thomas Bozza (Northwestern University, Chicago).

MouSensor Transgene

Using the M71 transgene backbone as described in Vassalli et al. (2002) and Rothman et al. (2005), including 485 bp of the M71 promoter upstream of the transcription start site (TSS) (Figure 1), we created a modular version of this transgenic vector such that any number of a 21-bp singular gene choice enhancer can be shuttled into the *NheI* site at position −485. Any OR CDS of interest can be cloned into the *AscI* site, and any IRES-Reporter cassette can be cloned into the *PacI* site. An internal ribosomal entry site (IRES) allows for bicistronic translation and simultaneous expression of a reporter gene. The transgenic animals that express the nx21-OR-IRES-Reporter transgenes are referred to as MouSensors. A detailed description of the x21 cloning strategy is provided in the Supplemental Experimental Procedures.

Genotyping

Presence of 4X21-M71-IRES-tauCherry transgene was assessed by PCR by scoring for the *tauCherry* gene with the following primers: FWD: 5′-CCCTGGA

CAACATCACAC-3′ and REV 5′-CCCTCCATGTGCACCTTGAAGCGCA-3′. To distinguish between hemi and homo 4•M71Cα animals, we used a real-time qPCR method that was previously described (D'Hulst et al., 2013). Presence of the M71-IRES-tauGFP gene-targeted allele was determined by using primers to detect *GFP*: FWD 5′-CCCTGGACAACATCACAC-3′ and REV 5′-CGTTTACGTCGCCGTCCAGCTC-3′ and primers to detect the WT *M71* allele with FWD 5′-CCGCACTGGACAAAACACTGAGGAG-3′ and REV 5′-CTGTTTCCTGTTCAGAGTTGGGTG-3′, allowing us to distinguish between WT, hemi, and homo animals.

Olfactometry

Odors (Sigma Aldrich) were delivered using a custom built olfactometer controlled by an Arduino board (https://www.arduino.cc/) with custom shields (http://mylabtime.blogspot.com) operating Teflon solenoids (Neptune Research) and connected to two mass flow controllers (Alicat Scientific) to dilute the clean air (N_2, max flow is 2 Lpm) and to dilute the odorized air (max flow is 300 SCCM). N_2 was used as the vapor carrier to avoid oxidation. Odor concentrations are expressed as % dilutions of saturated vapor and as molar saturated vapor concentration (μM s.v.), calculated using published vapor pressures at 25°C (US EPA, Estimation Programs Interface Suite, v.4.0 [Pacifico et al., 2012]). Flow diluted odors were delivered at 2 Lpm mixed prior to the delivery site with air odorized with varying dilutions of odorant taken from the saturated headspace of pre-cleaned amber vials with white polypropylene closures and septum (J.G. Finneran) containing 99% pure odorants. To avoid contamination of the olfactometer, odorized air was never passed through the Teflon valves. Instead, odors were mixed with N_2 in T-shaped mixing chambers (Neptune Research) and delivered to the animal's nose using an Arduino controlled vacuum system. Odorized streams carrying different odors did not come into contact. Output of the olfactometer was calibrated using the tracer odor Pinene and a photoionization detector (PID; Aurora Scientific).

In Vivo SpH Imaging

Mice 8–12 weeks old were anesthetized using Ketamine (100 mg/kg)/Xylazine (5 mg/kg) and maintained with Isoflurane (0.8% in O_2) and immobilized using a stereotactic head-holding device (Narishige). Optical signals for SpH and Cherry were recorded using an ANDOR Neo 5.5 sCMOS camera connected to a NIKON AZ100 epifluorescence microscope (NIS Elements) with a 4× objective (numerical aperture 0.4). Excitation wavelengths of 475 nm for SpH and 575 nm for Cherry and emission of 520 nm for SpH and 635 nm for Cherry were used to obtain images of the dorsolateral bulb through thinned skull overlaying the bulb of a freely breathing animal. Each imaging trial consisted of a pre-odor (3 s), odor (4 s), and post-odor (4 s) acquisition, with a total acquisition time per trial of 14 s (including 3 s of valve switch delay). Using serial code, the Arduino controlling the olfactometer was integrated in the NIS Elements software, so that the entire image acquisition sequence and flow-diluted odor delivery is controlled by the microscope's software (NIS Elements). Two-way ANOVA and Student's t tests were used for statistical analysis. Image processing is described in the Supplemental Experimental Procedures.

Olfactory Behavior Test

A two-bottle discrimination test was performed as previously described (Wysocki et al., 1977). Mice 8 weeks old were individually housed and given food ad libitum but restricted access to saccharin-phthalic acid solution (2.1×10^{-2} M sodium saccharin and 10^{-3} M phthalic acid [pH 6.5; SSPA]) for 1 hr twice a day for 2 days before the assay begins. This ensures mice would commence drinking the solution during the conditioning. On day 3 (conditioning day), mice are exposed to the SSPA solution with 10^{-4} dilution of odorized water for 10 min. Immediately after, they are injected with LiCl intraperitoneally (15 μl/g body weight of a 0.6 M solution) to induce the aversive malaise and lethargy state. After 2 hr, mice are returned to their home cage and given access to two bottles of drinking water; they are given the choice between SSPA solution containing a 10^{-4} dilution of the odor versus the non-odorized SSPA solution. During the following 3 days, every 24 hr, the location of the bottles is reversed and the concentration of the odorized solution is decreased to 10^{-6}, 10^{-7}, and 0.5×10^{-6}, respectively. Every day both bottles are weighed to determine the amount of liquid consumed. A PI was calculated as the amount of odorized solution consumed divided by the total amount of water solution consumed for each mouse for every 24-hr test period at each odor concentration. A t test was performed to test statistical significance, assuming two-tailed distribution and two-sample unequal variance. Values are mean ± SEM and are plotted on a log scale. Animals (both WT and transgenic) that did not seem to be conditioned after LiCl injections (showing a PI for 24dMACP higher than 20% at 10^{-4}) were excluded from our analysis (i.e., four WT and two homo). Student's t tests were used for statistical analysis of the data.

RNA Extraction and cDNA Synthesis

4•M71Cα hemi animals mice were sacrificed and the MOE tissue was dissected on a mixture of ice and dry ice. Tissue was snap frozen in liquid N_2 and stored at −80°C. RNA was isolated using the RNeasy Mini columns (QIAGEN, #74104) according the manufacturer's protocol. Tissue was homogenized in lysis buffer provided by the kit containing 10 μl β-mercaptoethanol. The concentrations of the isolated RNA samples were measured using a NanoDrop ND-1000 Spectrophotometer. After RNA extraction, an additional DNase digestion was performed with a TURBO DNA-free (Life Technologies, #AM1907) kit to remove all genomic DNA (gDNA) from the sample. First-strand cDNA was synthesized using SuperScript III First-Strand Synthesis System for RT-PCR (Life Technologies, #18080-051). First-strand cDNA was diluted 1:5 to a total volume of 100 μl. Refer to Supplemental Experimental Procedures for real-time qPCR.

Mitral Cell Labeling

Male YFP-g mice (strain: 014130, Jackson Laboratory) were crossed with female hemizygous 4•M71Cα (also *M71-GFP*$^{-/-}$) mice to generate compound mutant mice. Male offspring that were positive for both YFP and Cherry were euthanized at 8–12 weeks of age and OB tissue was processed for histological imaging. Images were collected on a LSM510 confocal microscope (Carl Zeiss) using objectives, Fluar, 10× N.A. 0.5, and PlanNeofluar 40× N.A.1.3.

SUPPLEMENTAL INFORMATION

Supplemental Information includes Supplemental Experimental Procedures, six figures, and five tables and can be found with this article online at http://dx.doi.org/10.1016/j.celrep.2016.06.047.

AUTHOR CONTRIBUTIONS

C.D. and P.F. designed the experiments and wrote the paper. C.D. and Y.S. conducted the in vivo imaging experiments. Y.S. wrote the MATLAB code. C.D., R.B.M., and A.C. performed the behavioral analysis. P.F., R.B.M., S.J., and Z.G. conducted the cryosectioning and imaging. C.D. and Z.G. conducted the quantitative real-time PCR experiments. D.T. performed genotyping during MouSensor derivation. S.J. performed the founder analysis. L. Bai and L. Belluscio conducted the mitral cell labeling and immunohistochemistry.

CONFLICTS OF INTEREST

C.D. and P.F. have filed a provisional patent on the MouSensor technology and have recently founded a company called MouSensor, LLC.

ACKNOWLEDGMENTS

We would like to thank the Hunter College Animal Facility Manager Barbara Wolin and Veterinarian Patricia Glennon for help in maintaining the transgenic colony and the Transgenic Core Facility at The Rockefeller University for generating transgenic founders. We would like to thank Dr. Thomas Bozza for helping set up SpH imaging and giving advice on the experiments. The development of the MouSensor technology was made possible by a Research Centers in Minority Institutions Program grant from the National Institute on Minority Health and Health Disparities (MD007599) of the NIH (SC1 GM088114), and its contents are solely the responsibility of the authors and do not necessarily represent the official views of the NIMHD or the NIH. Firmenich

sponsored other parts of the research. Z.G. is supported by the Hunter College HHMI UGRAD 52007535.

Received: August 5, 2015
Revised: May 2, 2016
Accepted: June 9, 2016
Published: July 7, 2016

REFERENCES

Belluscio, L., Lodovichi, C., Feinstein, P., Mombaerts, P., and Katz, L.C. (2002). Odorant receptors instruct functional circuitry in the mouse olfactory bulb. Nature *419*, 296–300.

Blauvelt, D.G., Sato, T.F., Wienisch, M., Knöpfel, T., and Murthy, V.N. (2013). Distinct spatiotemporal activity in principal neurons of the mouse olfactory bulb in anesthetized and awake states. Front. Neural Circuits *7*, 46.

Bozza, T., Feinstein, P., Zheng, C., and Mombaerts, P. (2002). Odorant receptor expression defines functional units in the mouse olfactory system. J. Neurosci. *22*, 3033–3043.

Bozza, T., McGann, J.P., Mombaerts, P., and Wachowiak, M. (2004). In vivo imaging of neuronal activity by targeted expression of a genetically encoded probe in the mouse. Neuron *42*, 9–21.

Bozza, T., Vassalli, A., Fuss, S., Zhang, J.J., Weiland, B., Pacifico, R., Feinstein, P., and Mombaerts, P. (2009). Mapping of class I and class II odorant receptors to glomerular domains by two distinct types of olfactory sensory neurons in the mouse. Neuron *61*, 220–233.

Bressel, O.C., Khan, M., and Mombaerts, P. (2016). Linear correlation between the number of olfactory sensory neurons expressing a given mouse odorant receptor gene and the total volume of the corresponding glomeruli in the olfactory bulb. J. Comp. Neurol. *524*, 199–209.

Bulfone, A., Wang, F., Hevner, R., Anderson, S., Cutforth, T., Chen, S., Meneses, J., Pedersen, R., Axel, R., and Rubenstein, J.L. (1998). An olfactory sensory map develops in the absence of normal projection neurons or GABAergic interneurons. Neuron *21*, 1273–1282.

Cheng, N., Bai, L., Steuer, E., and Belluscio, L. (2013). Olfactory functions scale with circuit restoration in a rapidly reversible Alzheimer's disease model. J. Neurosci. *33*, 12208–12217.

Chess, A., Simon, I., Cedar, H., and Axel, R. (1994). Allelic inactivation regulates olfactory receptor gene expression. Cell *78*, 823–834.

D'Hulst, C., Parvanova, I., Tomoiaga, D., Sapar, M.L., and Feinstein, P. (2013). Fast quantitative real-time PCR-based screening for common chromosomal aneuploidies in mouse embryonic stem cells. Stem Cell Reports *1*, 350–359.

Ebrahimi, F.A., and Chess, A. (2000). Olfactory neurons are interdependent in maintaining axonal projections. Curr. Biol. *10*, 219–222.

Feinstein, P., and Mombaerts, P. (2004). A contextual model for axonal sorting into glomeruli in the mouse olfactory system. Cell *117*, 817–831.

Feinstein, P., Bozza, T., Rodriguez, I., Vassalli, A., and Mombaerts, P. (2004). Axon guidance of mouse olfactory sensory neurons by odorant receptors and the beta2 adrenergic receptor. Cell *117*, 833–846.

Fleischmann, A., Shykind, B.M., Sosulski, D.L., Franks, K.M., Glinka, M.E., Mei, D.F., Sun, Y., Kirkland, J., Mendelsohn, M., Albers, M.W., and Axel, R. (2008). Mice with a "monoclonal nose": perturbations in an olfactory map impair odor discrimination. Neuron *60*, 1068–1081.

He, J., Wei, J., Rizak, J.D., Chen, Y., Wang, J., Hu, X., and Ma, Y. (2015). An odor detection system based on automatically trained mice by relative go no-go olfactory operant conditioning. Sci. Rep. *5*, 10019.

Kass, M.D., Rosenthal, M.C., Pottackal, J., and McGann, J.P. (2013). Fear learning enhances neural responses to threat-predictive sensory stimuli. Science *342*, 1389–1392.

Kraemer, S., and Apfelbach, R. (2004). Olfactory sensitivity, learning and cognition in young adult and aged male Wistar rats. Physiol. Behav. *81*, 435–442.

Liu, S., Shao, Z., Puche, A., Wachowiak, M., Rothermel, M., and Shipley, M.T. (2015). Muscarinic receptors modulate dendrodendritic inhibitory synapses to sculpt glomerular output. J. Neurosci. *35*, 5680–5692.

Magklara, A., Yen, A., Colquitt, B.M., Clowney, E.J., Allen, W., Markenscoff-Papadimitriou, E., Evans, Z.A., Kheradpour, P., Mountoufaris, G., Carey, C., et al. (2011). An epigenetic signature for monoallelic olfactory receptor expression. Cell *145*, 555–570.

Nguyen, M.Q., and Ryba, N.J.P. (2012). A smell that causes seizure. PLoS ONE *7*, e41899.

Pacifico, R., Dewan, A., Cawley, D., Guo, C., and Bozza, T. (2012). An olfactory subsystem that mediates high-sensitivity detection of volatile amines. Cell Rep. *2*, 76–88.

Rothermel, M., Carey, R.M., Puche, A., Shipley, M.T., and Wachowiak, M. (2014). Cholinergic inputs from Basal forebrain add an excitatory bias to odor coding in the olfactory bulb. J. Neurosci. *34*, 4654–4664.

Rothman, A., Feinstein, P., Hirota, J., and Mombaerts, P. (2005). The promoter of the mouse odorant receptor gene M71. Mol. Cell. Neurosci. *28*, 535–546.

Saito, H., Chi, Q., Zhuang, H., Matsunami, H., and Mainland, J.D. (2009). Odor coding by a Mammalian receptor repertoire. Sci. Signal. *2*, ra9.

Serizawa, S., Miyamichi, K., Nakatani, H., Suzuki, M., Saito, M., Yoshihara, Y., and Sakano, H. (2003). Negative feedback regulation ensures the one receptor-one olfactory neuron rule in mouse. Science *302*, 2088–2094.

Strotmann, J., Conzelmann, S., Beck, A., Feinstein, P., Breer, H., and Mombaerts, P. (2000). Local permutations in the glomerular array of the mouse olfactory bulb. J. Neurosci. *20*, 6927–6938.

Vassalli, A., Rothman, A., Feinstein, P., Zapotocky, M., and Mombaerts, P. (2002). Minigenes impart odorant receptor-specific axon guidance in the olfactory bulb. Neuron *35*, 681–696.

Vassalli, A., Feinstein, P., and Mombaerts, P. (2011). Homeodomain binding motifs modulate the probability of odorant receptor gene choice in transgenic mice. Mol. Cell. Neurosci. *46*, 381–396.

von der Weid, B., Rossier, D., Lindup, M., Tuberosa, J., Widmer, A., Col, J.D., Kan, C., Carleton, A., and Rodriguez, I. (2015). Large-scale transcriptional profiling of chemosensory neurons identifies receptor-ligand pairs in vivo. Nat. Neurosci. *18*, 1455–1463.

Wilson, R.I., and Mainen, Z.F. (2006). Early events in olfactory processing. Annu. Rev. Neurosci. *29*, 163–201.

Wysocki, C.J., Whitney, G., and Tucker, D. (1977). Specific anosmia in the laboratory mouse. Behav. Genet. *7*, 171–188.

Zhang, X., and Firestein, S. (2002). The olfactory receptor gene superfamily of the mouse. Nat. Neurosci. *5*, 124–133.

Zhang, J., Huang, G., Dewan, A., Feinstein, P., and Bozza, T. (2012). Uncoupling stimulus specificity and glomerular position in the mouse olfactory system. Mol. Cell. Neurosci. *51*, 79–88.